Insight into the kinematics of blue whale surface foraging through drone observations and prey data

Leigh G Torres [Corresp., 1] , Dawn R Barlow [1] , Todd E Chandler [2] , Jonathan D Burnett [3]

[1] Geospatial Ecology of Marine Megafauna Lab, Marine Mammal Institute, Department of Fisheries and Wildlife, Oregon State University, Newport, Oregon, United States

[2] Geospatial Ecology of Marine Megafauna Lab, Marine Mammal Institute, Oregon State University, Newport, Oregon, United States

[3] Aerial Information Systems Laboratory, Forest Engineering, Resources and Management, Oregon State University, Corvallis, Oregon, United States

Corresponding Author: Leigh G Torres
Email address: leigh.torres@oregonstate.edu

To understand how predators optimize foraging strategies, extensive knowledge of predator behavior and prey distribution is needed. Blue whales employ an energetically demanding lunge feeding method that requires the whales to selectively feed where energetic gain exceeds energetic loss, while also balancing oxygen consumption, breath holding capacity, and surface recuperation time. Hence, blue whale foraging behavior is primarily driven by krill patch density and depth, but many studies have not fully considered surface feeding as a significant foraging strategy in energetic models. We collected predator and prey data on a blue whale (*Balaenoptera musculus brevicauda*) foraging ground in New Zealand in February 2017 to assess the distributional and behavioral response of blue whales to the distribution and density of krill prey aggregations. Krill density across the study region was greater toward the surface (upper 20 m), and blue whales were encountered where prey was relatively shallow and more dense. This relationship was particularly evident where foraging and surface lunge feeding was observed. Furthermore, New Zealand blue whales also had relatively short dive times (2.83 ± 0.27 SE min) as compared to other blue whale populations, which became even shorter at foraging sightings and where surface lunge feeding was observed. Using an unmanned aerial system (UAS; drone) we also captured unique video of a New Zealand blue whale's surface feeding behavior on well-illuminated krill patches. Video analysis illustrates the whale's potential use of vision to target prey, make foraging decisions, and orient body mechanics relative to prey patch characteristics. Kinematic analysis of a surface lunge feeding event revealed biomechanical coordination through speed, acceleration, head inclination, roll, and distance from krill patch to maximize prey engulfment. We compared these lunge kinematics to data previously reported from tagged blue whale lunges at depth to demonstrate strong similarities, and provide rare measurements of gape size, and krill response distance and time. These findings elucidate

the predator-prey relationship between blue whales and krill, and provide support for the hypothesis that surface feeding by New Zealand blue whales is an important component to their foraging ecology used to optimize their energetic efficiency. Understanding how blue whales make foraging decisions presents logistical challenges, which may cause incomplete sampling and biased ecological knowledge if portions of their foraging behavior are undocumented. We conclude that surface foraging could be an important strategy for blue whales, and integration of UAS with tag-based studies may expand our understanding of their foraging ecology by examining surface feeding events in conjunction with behaviors at depth.

1 **Insight into the kinematics of blue whale surface foraging through drone observations and**
2 **prey data**

4 Leigh G. Torres[1], Dawn R. Barlow[1], Todd E. Chandler[2], Jonathan D. Burnett[3]

6 [1]Geospatial Ecology of Marine Megafauna Lab, Marine Mammal Institute, Department of
7 Fisheries and Wildlife, Oregon State University, 2030 SE Marine Science Drive, Newport,
8 Oregon, 97365, USA

9 [2]Geospatial Ecology of Marine Megafauna Lab, Marine Mammal Institute, Oregon State
10 University, 2030 SE Marine Science Drive, Newport, Oregon, 97365, USA

11 [3]Aerial Information Systems Laboratory, Forest Engineering, Resources and Management,
12 Oregon State University, 280 Peavy Hall, Corvallis, Oregon, 97331 USA

14 Corresponding author:
15 Leigh Torres[1]
16 Hatfield Marine Science Center
17 2030 SE Marine Science Drive
18 Newport, OR 97365, U.S.A
19 leigh.torres@oregonstate.edu

Abstract

24   To understand how predators optimize foraging strategies, extensive knowledge of predator
25   behavior and prey distribution is needed. Blue whales employ an energetically demanding lunge
26   feeding method that requires the whales to selectively feed where energetic gain exceeds
27   energetic loss, while also balancing oxygen consumption, breath holding capacity, and surface
28   recuperation time. Hence, blue whale foraging behavior is primarily driven by krill patch density
29   and depth, but many studies have not fully considered surface feeding as a significant foraging
30   strategy in energetic models. We collected predator and prey data on a blue whale (*Balaenoptera*
31   *musculus brevicauda*) foraging ground in New Zealand in February 2017 to assess the
32   distributional and behavioral response of blue whales to the distribution and density of krill prey
33   aggregations. Krill density across the study region was greater toward the surface (upper 20 m),
34   and blue whales were encountered where prey was relatively shallow and more dense. This
35   relationship was particularly evident where foraging and surface lunge feeding was observed.
36   Furthermore, New Zealand blue whales also had relatively short dive times (2.83 ± 0.27 SE min)
37   as compared to other blue whale populations, which became even shorter at foraging sightings
38   and where surface lunge feeding was observed. Using an unmanned aerial system (UAS; drone)
39   we also captured unique video of a New Zealand blue whale's surface feeding behavior on well-
40   illuminated krill patches. Video analysis illustrates the whale's potential use of vision to target
41   prey, make foraging decisions, and orient body mechanics relative to prey patch characteristics.
42   Kinematic analysis of a surface lunge feeding event revealed biomechanical coordination
43   through speed, acceleration, head inclination, roll, and distance from krill patch to maximize
44   prey engulfment. We compared these lunge kinematics to data previously reported from tagged
45   blue whale lunges at depth to demonstrate strong similarities, and provide rare measurements of
46   gape size, and krill response distance and time. These findings elucidate the predator-prey
47   relationship between blue whales and krill, and provide support for the hypothesis that surface
48   feeding by New Zealand blue whales is an important component to their foraging ecology used
49   to optimize their energetic efficiency. Understanding how blue whales make foraging decisions
50   presents logistical challenges, which may cause incomplete sampling and biased ecological
51   knowledge if portions of their foraging behavior are undocumented. We conclude that surface
52   foraging could be an important strategy for blue whales, and integration of UAS with tag-based
53   studies may expand our understanding of their foraging ecology by examining surface feeding
54   events in conjunction with behaviors at depth.

55

Introduction

57   Optimal foraging theory predicts that predators maximize energetic gain by choosing to exploit
58   prey so that caloric intake outweighs energetic costs of search, capture and digestion (Charnov
59   1976). Foraging marine mammals must also include oxygen consumption, breath holding
60   capacity, and surface recuperation time in this energetic balance. Yet, application of optimal
61   foraging theory in marine systems can be challenging due to often obscured knowledge of prey
62   availability and predator behavior. As the largest predator on earth, the blue whale (*Balaenoptera*
63   *musculus*) has massive prey requirements to meet energy demands (Williams *et al.* 2001). Hence,

64 their foraging ecology must be efficient and optimized through adaptable feeding strategies
65 primarily relative to prey patch depth and density (Croll *et al.* 2001, Doniol-Valcroze *et al.* 2011,
66 Goldbogen *et al.* 2011, Goldbogen *et al.* 2013a, Goldbogen *et al.* 2015, Hazen *et al.* 2015,
67 Friedlaender *et al.* 2016), while also maintaining dependence on the surface for oxygen supply.
68 This tie to the surface has led to the successful application of central place foraging theory
69 (Orians 1979) to blue whale foraging behavior, with both surface recuperation and foraging
70 times increasing with target prey patch depth (Doniol-Valcroze *et al.* 2011).

71 Blue whales are rorqual whales that employ a lunge feeding method where the whale accelerates
72 forward rapidly and opens it jaws to engulf prey-laden water into an extensible buccal cavity that
73 is then filtered through baleen plates (Goldbogen *et al.* 2017). Lunge feeding is energetically
74 demanding due to body acceleration, engulfment and acceleration of water mass, and drag
75 forces, all of which deplete oxygen stores and limit dive duration (Acevedo-Gutierrez *et al.*
76 2002, Potvin *et al.* 2010, Goldbogen *et al.* 2012). Hence, for lunge feeding to be energetically
77 efficient whales must locate and engulf high-density prey patches so to maximize energy gain.
78 Blue whales lunge feed at depths ranging from the surface to over 300 m (Doniol-Valcroze *et al.*
79 2011, Hazen *et al.* 2015) and are specialized predators of krill, which are ephemeral and patchy
80 (Schoenherr 1991, Croll *et al.* 2005, Goldbogen *et al.* 2011, Hazen *et al.* 2015, Nickels *et al.*
81 2019). Therefore, blue whales must forage selectively by targeting dense prey aggregations that
82 compensate for the energetic cost of lunging and diving (Doniol-Valcroze *et al.* 2011, Hazen *et*
83 *al.* 2015).

84 The ecology and energetics of blue whale foraging has been illuminated through multiple studies
85 that analyzed data acquired from animal-borne tags applied to whales in southern California,
86 USA (Goldbogen *et al.* 2011, Goldbogen *et al.* 2012, Goldbogen *et al.* 2015, Hazen *et al.* 2015,
87 Friedlaender *et al.* 2016). These studies demonstrate that blue whales modulate lunge feeding
88 rates as a function of prey patch density and depth to optimize energetic efficiency (Goldbogen
89 *et al.* 2011, Hazen *et al.* 2015). A detailed kinematic analysis of blue whale lunge feeding
90 estimated the energetic costs, gains, and efficiency of a single lunge at the surface and multiple
91 lunges at depth (Goldbogen *et al.* 2011). In both scenarios energy gained from engulfed krill
92 exceeded energetic costs, yet results indicate that a single surface lunge is 2.5 times more
93 energetically efficient than multiple (3.5) lunges conducted during a dive to depth (200 m).
94 Hence, based on optimal foraging theory, a blue whale should only feed at depth when relative
95 krill density at depth exceeds surface density so that the energetic costs of diving are offset.
96 Additionally, models of blue whale foraging efficiency based on tag data demonstrated that
97 foraging at depth only exceeds the net energy gain of surface feeding when krill density at depth
98 is > 3 times surface densities (Goldbogen *et al.* 2011). This scenario may be typical of target
99 prey in the southern California ecosystem (*Euphausia pacifica*; *Thysanoessa spinifera*) that
100 demonstrate strong diel cycles (Croll *et al.* 2005) and association with bathymetric features
101 (Schoenherr 1991, Nickels *et al.* 2019), but possibly not of other krill species targeted by blue
102 whales in other ecosystems.

103 Blue whale surface lunge feeding (SLF) is commonly observed in many ecosystems (Schoenherr
104 1991, Gill 2002, Doniol-Valcroze *et al.* 2011, Kot *et al.* 2014, Buchan and Quiñones 2016), and
105 may be an important foraging strategy for blue whales as an alternative to energetically
106 demanding deep foraging, particularly in ecosystems where krill are distributed more evenly

107   vertically through the water column or biased toward the surface. Indeed, when lunges at depth
108   and the surface were both assessed in tag data and incorporated into a central place foraging
109   model applied to blue whales feeding in St. Lawrence River, Canada, predicted dive efficiency
110   was highest at the surface and declined steadily with depth (Doniol-Valcroze *et al.* 2011). High
111   rates of surface foraging by humpback whales (*Megaptera novaeangliae*) have also been
112   documented (Friedlaender *et al.* 2009, Ware *et al.* 2011, Owen *et al.* 2017), even when prey
113   density was greater at depth (Goldbogen *et al.* 2008). While rorqual surface feeding has been
114   observed and reported, quantitative description and comparison of whale surface kinematics are
115   often excluded from accelerometer tag data analysis due to biomechanical processes and forces
116   that restrict accurate algorithmic detection of lunges at the surface (Allen *et al.* 2016, Owen *et al.*
117   2016). Hence, biomechanic description of lunge feeding has focused on deep foraging dives and
118   surface lunging is relatively poorly understood (Allen *et al.* 2016).

119   In New Zealand and southern Australia, pygmy blue whales (*B. m. brevicauda*) feed on a coastal
120   krill species (*Nyctiphanes australis*) known for its surface swarming behavior and lack of diel or
121   depth patterns relative to density and biomass (O'Brien 1988, Young *et al.* 1993). Given the
122   energetic costs of diving, and shallow or homogenously distributed prey, blue whales in these
123   ecosystems should preferentially feed near the surface. Some evidence for this expectation is
124   available from southern Australia where krill surface swarms were associated with 48% of blue
125   whale sightings, with frequent observation of surface and sub-surface feeding from aerial
126   surveys (Gill 2002). Thus, disregard of blue whale surface feeding may bias our understanding of
127   their foraging ecology and hinder conservation efforts in some ecosystems. Due to the context
128   dependence of blue whale response to disturbance events based on behavioral state (Goldbogen
129   *et al.* 2013b) and prey availability (Friedlaender *et al.* 2016), efforts to de-couple the 3-D overlap
130   of whales and anthropogenic impacts should consider the functional habitat use of blue whales
131   through the whole water column. For instance, blue whales demonstrate an increased response to
132   shipping traffic when at the surface (McKenna *et al.* 2015).

133   Blue whale SLF events are a dramatic predation spectacle leading to multiple descriptions
134   (Fiedler *et al.* 1998, Corkeron *et al.* 1999, Gill 2002, Kot *et al.* 2014, Buchan and Quiñones
135   2016), but surface feeding behavior has rarely been incorporated into our understanding of their
136   optimal foraging strategies, with the exception of Doniol-Valcroze *et al.* (2011) and Goldbogen
137   *et al.* (2011), both of which indicate the high net energetic gain of surface feeding. Therefore,
138   incomplete quantification of surface feeding behavior, either deliberate or due to data limitations,
139   can limit or bias understanding of how blue whales make optimal foraging trade-offs between
140   prey depth and density, which are likely a function of ecological context and allometric scale. In
141   this study, we examine concurrent data on krill availability and blue whale distribution within a
142   newly described foraging area in New Zealand (Torres 2013, Barlow *et al.* 2018) to examine the
143   relationships between prey depth and density and whale dive times and behavior. We consider
144   these data within previously described blue whale foraging efficiency (Goldbogen *et al.* 2011)
145   and optimality (Doniol-Valcroze *et al.* 2011) models, and posit that surface feeding among these
146   relatively diminutive blue whales in this ecosystem is a significant foraging strategy that
147   maximizes their energetic gain. Additionally, we analyze four blue whale surface foraging events
148   captured via Unmanned Aerial System (UAS) to demonstrate the utility of drones to provide
149   novel and detailed data on whale kinematics, sensory use, and decision making. We provide a
150   quantitative kinematic description of a blue whale 'lateral lunge feeding' surface event

151   (Goldbogen *et al.* 2006, Kot *et al.* 2014), where the whale rotates > 90° along its longitudinal
152   axis to engulf a krill patch, and compare this description to reports of blue whale lunge feeding
153   events at depth recorded via tag data (Goldbogen *et al.* 2011, Goldbogen *et al.* 2013a, Goldbogen
154   *et al.* 2015, Cade *et al.* 2016, Friedlaender *et al.* 2017). Additionally, this footage is unique due
155   to the well-illuminated krill patch, allowing assessment of predator and prey simultaneously. We
156   suggest that UAS can complement tagging efforts by providing quantitative data on surface
157   foraging behavior from a new perspective (Torres *et al.* 2018), allowing a more complete
158   description of blue whale foraging strategies.

159   **Materials & Methods**

160   **Data collection**: Fieldwork was conducted in February 2017 on a blue whale foraging ground in
161   the South Taranaki Bight (STB) region of New Zealand (Fig. 1; Barlow *et al.* 2018) where
162   whales target aggregations of *N. australis*. Blue whale occurrence data was collected during
163   standardized survey effort (Barlow *et al.* 2018) aboard a 19.2 m vessel at speeds of 8 to 12 knots
164   in suitable weather conditions (Beaufort Sea State <5). Survey observation data was collected at
165   4 m above the waterline by two observers scanning either the port or starboard sides of the
166   trackline independently. Survey tracklines did not follow a standardized layout (i.e., sawtooth or
167   grid pattern lines), but rather aimed to maximize encounter rates with blue whales and therefore
168   had an irregular trackline pattern directed toward productive (based on remotely sensed images
169   of chlorophyll-*a* and sea surface temperature) or previously unsurveyed areas. Survey effort
170   stopped at all sightings of blue whales and the whale(s) was slowly approached for behavioral
171   observation. Whale behavior states were classified as travel, forage, social, rest, or unknown
172   based on observations, with further details, such observations of SLF events, noted. Travel was
173   defined as directional movement and regular surfacing. Indications of foraging included surface
174   lunges and staying in one area for a prolonged period with irregular surfacings or fluke-out dives.
175   Social behaviors included mother-calf nursing, prolonged coordinated surfacing such as racing,
176   and tactile contact between individuals. Resting behavior consisted of logging near the surface
177   with minimal forward movement. All behaviors that did not fit within these classifications were
178   considered unknown. Dive times of individual whales at all sightings were recorded as the
179   interval of time between the whale's surfacings. The mean dive time was attributed to the
180   sighting. If multiple individuals were present, dive times were recorded for each individual
181   whale, with an average dive time calculated per whale, and then a group mean was determined
182   for that sighting. During survey effort and at many whale sightings, krill distribution data was
183   collected by a Simrad EK60 echosounder. Field research on blue whales was conducted under
184   research permit approval from the New Zealand Department of Conservation (45780-MAR) and
185   Institutional Animal Care and Use Committee exemption from Oregon State University (16-
186   1083).

187   A DJI Phantom 4 Advanced (non-Pro) UAS was flown over blue whales using manual flight
188   control and real time camera output for the primary purpose of body morphometric assessment
189   through photogrammetry (Burnett *et al.* 2018). The UAS camera had a 3.61 mm focal length and
190   a 0.0015 mm pixel size. On 20 February 2017 at 19:21 local time the UAS was hand-launched
191   off the research vessel to fly over a single blue whale. Conditions were exceptional, with no wind
192   or swell, and bright off-angle lighting, which enhanced water clarity and contrast so that multiple
193   surface patches of krill were identifiable. The UAS was navigated toward the whale's location
194   after collecting calibration data over a board of known length at multiple altitudes for the

195   purpose of later correcting the barometric altimeter (Burnett *et al.* 2018). Just after the whale was
196   localized in the UAS video with camera pointing nadir, the whale began a SLF event (Table 1,
197   Event 1 at 19:23:38). The UAS operator navigated the drone to film the event as best as possible
198   given the rapid sequence of events, yet unfortunately the expanded buccal cavity is out of frame
199   for ~1.5 sec during engulfment of the krill. Although the whale dove out of sight after this
200   feeding event, we later filmed its surface activity for another 5:47 min using the UAS. The UAS
201   maintained an altitude between 29 and 38 m above the whale during these observations while we
202   recorded three other instances of this same blue whale recognizing surface krill patches but not
203   feeding (Table 2). Low UAS battery power and the setting sun forced retrieval of the UAS. A
204   small tissue biopsy sample was then collected from the whale using a lightweight biopsy dart
205   (Krützen *et al.* 2002) for genetic analysis to determine sex (Barlow *et al.* 2018).

206   **Krill data analysis.** Hydroacoustic data were collected using a Simrad ES120 splitbeam
207   transducer with a 120 kHz receiver, 250 W, 1.024 ms pulse length, and 0.5 s ping rate. The
208   transducer was mounted on a pole and deployed 1.45 m below the surface. Raw data were
209   processed and extracted using the MATLAB-based program ESP3 (Ladroit 2017), developed for
210   fisheries hydroacoustic analysis. Volume backscattering (Sv) measurements were binned
211   vertically into 1 m depth bins and horizontally into 5-ping bins. The upper 2 m of the water
212   column were excluded due to noise from disturbances at the surface such as wind and swell, and
213   sections with recognizable interference from CTD casts or missed pings were removed.
214   Following complete visual inspection of the echograms for quality control, measurements made
215   at 2 m or deeper were retained for analysis. The echosounder was not calibrated, and therefore all
216   values for backscatter strength represent a relative characterization of prey availability within
217   this ecosystem.
218
219   Zooplankton-like schools were identified by excluding ping data with volume backscattering
220   strength below the −90 dB threshold at 120 kHz. We are confident that this threshold reliably
221   identified and captured aggregations visible on the echosounder, thereby effectively
222   characterizing schools within this ecosystem. The threshold value applied is more conservative
223   than those used in a similar analysis for larger krill species with established cutoff frequencies
224   (*e.g., Euphausia superba*, Bernard & Steinberg 2013). Recognizing that we were not able to
225   definitively exclude other ensonified species (*i.e.*, fish) and in the absence of a known target
226   strength for the krill species of interest (*N. australis*), we assume that the aggregations identified
227   acoustically were predominately comprised of krill. Krill aggregations were identified following
228   the methods described by Bernard *et al.* (2017). Each element in the acoustic matrix that
229   qualified as krill was considered to be part of an "aggregation" if one of its eight neighboring
230   elements also qualified as krill (Lawson *et al.* 2008, Bernard and Steinberg 2013).

231   The mean Sv, depth, and vertical thickness were calculated for each krill aggregation
232   (Supplementary Information, Table S1, Fig. S1). Mean depth was defined as the depth at the
233   midpoint of each aggregation. Mean Sv of each aggregation was used to represent patch density.
234   Aggregations were defined as being at a blue whale sighting if the center of the aggregation was
235   within a 2 km radius of the blue whale sighting, and all other krill aggregations were considered
236   not to be at a blue whale sighting. A threshold of 2 km was applied because blue whale sightings

237   ranged up to 2 km from the initial sighting location; hence, this distance was considered to best
238   characterize the availability of krill aggregations to the whale(s) at a sighting.

239   Krill patch density observed during the four UAS filmed events could not be quantitatively
240   determined because the underwater portion of the patches are indiscernible. Yet, density of
241   surface swarms of *N. australis* can range between 3000 and > 450,000 ind. m^{-3}, with individual
242   krill lengths 15-18 mm and the wet weight biomass ranging between 40 g m^{-3} and 7 kg m^{-3}
243   (O'Brien 1988). Furthermore, O'Brien (1988) estimated the wet weight of a 15 m cigar-shaped
244   patch of *N. australis* to be 100 kg. The length of the krill patch consumed during the filmed SLF
245   event was 16.2 m (excluding the long tail on the bottom-right: Fig. 2h). Therefore, although we
246   cannot quantify the density or biomass of the patch targeted during the SLF event, both metrics
247   may be relatively high.

248   **UAS video of analysis of blue whale.** Despite not having a laser altimeter on-board our UAS,
249   accurate scaling between pixels and metric units of images captured in nadir was achieved using
250   our calibration board (Dawson *et al.* 2017, Burnett *et al.* 2018). Barometric altitude was
251   corrected for bias using pixel length (from video) and metric length measurements of the board
252   at a range of altitudes to create a correction model (Burnett *et al.* 2018). Measurements were
253   scaled from pixels to metric units by multiplying pixel measurements by the ground sampling
254   distance (GSD) where GSD was calculated by multiplying model corrected barometric altitude
255   by camera sensor pixel size in mm and dividing by camera focal length in mm (Comer *et al.*
256   1998).
257
258   In all four events, estimates of the whale's position relative to the krill patch were reconstructed
259   from the UAS video sequence using Adobe Photoshop CC (V 2015.5; hereafter Photoshop). At
260   0.5 second intervals, the following metrics were estimated: horizontal distance between the
261   whale's rostrum tip and the krill patch, instantaneous speed of the whale, instantaneous
262   acceleration of the whale, and the whale's body roll and head inclination angle. Also estimated
263   were the distance at which the krill responded to the whale, krill patch area pre-strike, and krill
264   patch area post-strike for the SLF event. The lack of reference points in the relatively
265   homogenous ocean scene was a challenge for data analysis, however we attempted to mitigate
266   this issue by using a consistent point on the leading edge of the krill patch as a reference marker
267   (anchor point) and limiting data analysis to when the whale and krill were simultaneously
268   visible. We therefore assume that the krill patch did not move significantly relative to the
269   whale's larger magnitude movements until its flee response from the whale at close range, which
270   was also measured using the same anchor point to ensure consistency. We also assume no impact
271   of water current on data analysis, which is considered a valid assumption as minimal lateral
272   movement of the krill was observed during periods when the aircraft was stationary. Our
273   estimated values of relative acceleration and speed should not be considered absolutes due to the
274   many sources of minor uncertainty in UAS imagery that are difficult to quantify given the lack of
275   reference points, *in situ* water current measurements, and ability to estimate error. However, our
276   methods provide reasonable estimates of whale kinematics as confirmed by similarities to tag-
277   derived metrics of blue whale lunge biomechanics, provide rare estimates of krill prey flee
278   response, and are consistent across the four UAS filmed foraging events thus providing reliable
279   relative comparisons between events. For future applications of UAS to film whale surface

280   behavior we suggest the use of a laser altimeter to improve precision and accuracy of altitude
281   estimates, and thus speed and acceleration measurements.
282
283   During the SLF event, time-stamps of fluke beats, pectoral fin movements, and mouth opening
284   were also noted, and maximum gape was calculated using the online tool at
285   https://www.ginifab.com/feeds/angle_measurement/. The times determined as when the whale
286   first responds to krill patch, krill begin flee response to whale, and of widest gape during the SLF
287   event are recognized as subjective choices, yet all authors estimated these values independently
288   and were in agreement.
289
290   The interval of interest in Event 1 when the SLF event was filmed was isolated using the video
291   timeline functionality in Photoshop to the time frame beginning immediately before the whale
292   changes directions in response to the krill patch and ending at the completion of the dive
293   following the SLF event. This interval limited the analysis to frames between 135.37 s to 166.87
294   s and corresponds to 12 seconds pre-strike through 19.5 seconds post-strike. Video of the lunge
295   feeding event was segmented into 3,840 x 2,160 pixel images at 0.5 second intervals using the
296   video rendering function in Photoshop. Images were distortion corrected in MATLAB™
297   (Burnett *et al.* 2018) and mosaicked in Photoshop. To preserve image scale of the mosaic, a new
298   15,000 by 15,000 pixel blank image was generated with the same dots per inch (DPI) as the
299   distortion-corrected images. Estimation of the whale's relative speed and acceleration during the
300   SLF event was limited to the time interval where the krill patch and whale were in the frame
301   simultaneously from 9 s pre-strike to 19.5 s post-strike. These 0.5 sec interval images were
302   imported and spatially arranged using the krill strike point as the anchor position. Whale position
303   with respect to time was estimated by recording the x, y coordinates of the tip of the whale's
304   rostrum position in each of the constituent images within the mosaic.

305   Distance at 0.5 second intervals was estimated using the x, y position at the beginning and end of
306   each interval as inputs to the Euclidian distance equation. Distances were scaled to units of
307   meters using the GSD equation (Burnett *et al.* 2018). The 3.61 mm focal length camera on a
308   Phantom 4 Advanced at 29.5 m mean corrected altitude above-sea level resulted in a 0.0119 m
309   GSD per pixel scaling constant. A spline function of distance with respect to time was developed
310   by accumulating distance over time using the 'Spline' function in R (V 3.4.3) (R Development
311   Core Team 2018). The spline function allowed for the estimation of instantaneous speed and
312   instantaneous acceleration. A spline was selected instead of using raw numbers to estimate
313   average speed and acceleration over small time intervals in an effort to reduce the inherent
314   noisiness of the data due to small errors associated with scaling and imprecision associated with
315   visual interpretation. Speed was estimated instead of velocity because we were interested in
316   accumulated distance instead of vector-dependent total displacement. Distance between the
317   whale and krill patch was estimated by calculating the scaled pixel distance between the tip of
318   the whale's rostrum position and initial krill strike point at each time interval.

319   Following the mosaic, images associated with the undisturbed pre-strike krill patch were merged
320   to facilitate contiguous area estimate (Fig. 2h). Post-strike residual krill patch was estimated
321   using the frame at 151.87 s that displays the entire residual krill patch (Fig. 2i). Scaling of pixel
322   areas to square meters occurs using the 0.0119 m scalar.

323   Individual images at 0.5 sec intervals during Event 1 were visually assessed by all four co-
324   authors independently to subjectively assess roll and head inclination throughout the SLF event.
325   Body roll analysis began at 12 seconds pre-strike and was evaluated using the right-hand rotation
326   convention where rotation to the left is negative and rotation to the right is positive (Fig. S2 in
327   Supplementary Information). 0° body roll occurs when the whale is swimming straight with the
328   body level in the water. The position of the whale's spine, pectoral fins, jaw line, and body
329   flanks relative to the overhead perspective of the UAS camera in nadir were used to estimate the
330   whale's body roll. Head inclination is the measure of angular head position deviation from
331   neutral where neutral (0°) occurs when the body is fully elongated with a neutral spine and an
332   imaginary straight line extends from the tip of the rostrum to the tail. Head inclination ranges
333   from 90° to -90° where positive is a position where the head is above the imaginary line
334   connecting the rostrum and tail, and negative is the position below the imaginary line connecting
335   the rostrum and tail. Change in head inclination is best observed at roll angles with absolute
336   values between 45º and 110º, so estimations were limited to between 4 sec pre- to 7.5 post-strike
337   (unless unobservable between 2.5 and 3.5 sec post-strike when the whale was off-screen; Fig. 2a,
338   2j-l).

339   Subjective visual estimation of head inclination and roll angles by each co-author is imprecise
340   but indicative of relative body attitude changes with respect to time. Interpretation of head
341   inclination and roll was limited to 5º and 10º increments, respectively, to reflect the imprecision
342   of the estimates (Fig. S2 in Supplementary Information). Moreover, we calculated the Interrater
343   Correlation Coefficient (ICC; Koo and Li 2016) between the four independent evaluations of
344   head inclination and roll by co-authors to evaluate consistency and absolute-agreement as
345   metrics of confidence in estimations. ICC estimates and their 95% confident intervals were
346   calculated using the 'PSYCH' statistical package in R based on a mean-rating (k = 4 raters),
347   estimating consistency and absolute-agreement, using a 2-way mixed-effects model. The mean
348   and CV values of the four head inclination and roll estimates for each 0.5 sec interval image
349   were used in Fig. 2a to illustrate the blue whale's body positioning throughout the SLF event,
350   and any variation in estimations.

351

352   **Results**

353   **Distribution of blue whales and krill.** During 887 km of survey effort in the South Taranaki
354   Bight (STB) of New Zealand, 32 blue whale sightings were recorded of 68 individuals (Fig. 1).
355   Foraging behavior was apparent at 15 sightings, with SLF observed at six of those sightings.
356   Echosounder data were recorded for 90.6 h during the field season and 2,911 krill aggregations
357   were identified from analysis of these data. The highest krill density occurred in the upper 20 m
358   of the water column, and blue whale sightings with perceived foraging behavior occurred in
359   habitats with greater krill density relative to background availability (Fig. 3). Furthermore, the
360   mean depth of krill aggregations was shallower at all blue whale sightings as compared to
361   background availability, and depth became progressively shallower when compared to sightings
362   where foraging behavior was detected or SLF was observed (Table 2, Fig. 3). The dive times of
363   New Zealand blue whales followed this same trend, with relatively short dive times recorded for

364 all sightings (2.83 ± 0.27 SE min), which became even shorter at apparent foraging sightings and
365 where SLF was observed (Table 2). Krill aggregation depth and density during the sighting of
366 the UAS filmed whale are representative of the general pattern of krill availability across the
367 study region (Fig. 3), thus supporting the interpretation of these filmed surface behaviors relative
368 to the study area and whale population.

369 **Kinematics of the UAS filmed surface lunge feeding event.** An 18.69 m female blue whale –
370 determined through photogrammetry (Burnett *et al.* 2018) and genetics (Barlow *et al.* 2018)
371 respectively – was filmed via UAS engaged in four surface foraging events (Table 1), including a
372 successful SLF event. Kinematic analysis of this SLF event (Event 1, Table 1) reveals dynamic
373 maneuvers by the whale in speed, acceleration, head inclination and roll to line up the prey for
374 maximum engulfment (Fig. 2). The ICC and reliability ratings of the four independent
375 estimations by each co-author of the whale's head inclination and roll in 0.5 sec interval images
376 found that roll estimates were estimated with excellent reliability, and head inclination estimates
377 were estimated with moderate to excellent reliability (Table S2 in Supplemental Information).
378 These results are also reflected in the low CV in Fig. 2a, all of which indicate high confidence in
379 head inclination and roll estimates.

380 Initially the whale is travelling fast (2.8 m s^{-1}) 9.0 s before the strike, then slows down when she
381 recognizes the krill patch at a distance of 20.74 m and begins her pre-lunge roll to her left side
382 (min roll angle -27.5°) to line-up the patch. Then she performs one full fluke beat cycle while
383 rolling onto her right side (max roll angle 110°), and reaches maximum relative acceleration of
384 5.8 m s^{-2} 1 s before strike, followed by maximum downward head inclination (-15°) 0.5 s before
385 strike just as her mouth is beginning to open. At strike, her mouth begins to open while at a
386 maximum relative speed of 3.33 m s^{-1}, and reaches its widest gape angle of 33° 1.5 s after strike
387 (Fig. 2g) when maximum upward head inclination (18.75°) and maximum deceleration (3.7 m s^{-2})
388 occurs. The duration of the lunge event, from mouth opening to mouth closure, is 4.14 sec. The
389 whale then rolls back to center and descends slowly (mean relative speed 1.22 m s^{-1}) without
390 taking another breath until she surfaces 2:26 min after her previous breath. The whale's surface
391 series prior to the SLF event included breaths 54, 38 and 18 seconds before strike.

392 The UAS footage also enables observation of fluke and pectoral fin movements relative to the
393 foraging mechanics of a SLF event. The observed whale gets up to speed with two complete
394 fluke cycles (4 beats): the first cycle is used during pre-lunge roll maneuvering for target patch
395 line-up; the second fluke cycle accelerates the whale toward the patch; she stops fluking at strike,
396 and then glides down with small fluke beats starting 9.5 s after strike. The whale flares her left
397 pectoral fin upwards 0.5 s before strike, and then lays the fin against her enlarged buccal cavity
398 after strike; both pectoral fins remain extended to her sides as she descends like an airplane.

399 **Predator and prey behavior**. While we are unable to calculate prey patch volume in cubic
400 meters, the estimated area of the krill patch before and after the SLF event is 45 and 32 m^2
401 respectively, although some krill may also be under the whale after the lunge event (Fig. 2h-i).
402 Reduced krill patch density is visually evident after the SLF event based on differences in color
403 and saturation (Fig. 2h-i). Surface krill in the target patch begin to respond to the SLF predation
404 event when the whale is 2 m away, at 0.8 s before strike, perhaps due to the pressure wave from

405 the whale's rostrum (krill at depth not evaluated; Fig. 2e). At this time, the whale is moving fast
406 (~3 m s^{-1}), likely to overcome the rapid escape maneuvers of krill (O'Brien 1987). The UAS
407 footage allows observation of individual krill 'uncoordinated tail-flips', group 'flash expansion',
408 and propagation of escape response (Fig. 2f) through the krill swarm as described by O'Brien
409 (1987). Although the krill move in response to the predatory whale, the distance traveled is small
410 relative to the speed and size of the whale's gape. Indeed, the krill do not appear to flee in an
411 outward direction from the patch and the general shape of the patch, including the long "tail", is
412 maintained throughout the lunge (UAS videos available in Supplemental Information). This lack
413 of prey dispersion likely allows a high capture percentage for the lunging whale.

414 During all four UAS filmed events, the blue whale appears to use her right eye to gain visual
415 information about krill patch size, density and orientation to inform her decisions (Fig. 4; UAS
416 videos available in Supplemental Information). For example, prior to the whale's right side roll
417 for the SLF event, she performs a pre-lunge roll to her left allowing her right eye to observe the
418 krill patch at a distance of 18.46 m 6.5 s before strike (Fig. 2d).

419

Discussion

420 **Discussion**

421 Based on our comparative analysis of echosounder prey data and the corresponding distribution
422 of blue whales, it appears that New Zealand blue whales during the study period responded to the
423 distribution of their prey by preferentially foraging in habitat with dense, surface-oriented krill
424 aggregations. Furthermore, the short dive times of New Zealand blue whales reflects this shallow
425 krill distribution and contrasts dive times reported for blue whales feeding in southern California
426 (9.8 ± 1.8 min) where krill aggregations are much denser at depth (Goldbogen *et al.* 2011). These
427 results indicate that blue whales in the STB of New Zealand take advantage of shallow krill
428 aggregations, similar to the findings of Schoenherr (1991) that documented increased density of
429 surface krill swarms near surface foraging blue whales in Monterey Bay canyon, CA, USA.
430 Results from both studies demonstrate that foraging blue whales minimize the energetic expense
431 of diving and oxygen consumption when possible, thus aligning with the theory that diving
432 predators should forage close to the surface when possible (Kramer 1988). Therefore,
433 comprehensive assessments of blue whale foraging ecology and energetics in ecosystems with
434 surface krill aggregations should include surface foraging behavior. Although our sample size of
435 UAS filmed foraging events is very low (n = 4 events), video analysis demonstrates the utility of
436 this observation and data collection method for documentation of blue whale surface behavior.
437 The kinematic results from the UAS video analysis of the SLF event are comparable to data
438 derived from accelerometer and camera tags deployed on blue whales feeding at depth, and
439 provides rare information, such as krill response, change in prey patch size after a SLF event,
440 and potential use of visual cues to inform foraging decisions.

441 Compared to published speed profiles of blue whale lunges at depth derived from tag
442 deployments in southern California (Goldbogen *et al.* 2011), our kinematic analysis of the UAS
443 filmed SLF event by a New Zealand blue whale produced estimates that fit within the average
444 range of approach speed, strike speed, and post-strike speed. Additionally, our results illustrate

445   that peak speed coincided with mouth opening (strike), and peak deceleration coincided with
446   maximum gape, both of which match camera tag-derived results (Cade *et al.* 2016). These
447   kinematic similarities are interesting considering the smaller size of the New Zealand blue whale,
448   relatively small gape opening used (33° compared to ~80° for five southern California blue
449   whales; Potvin *et al.* 2010, Goldbogen *et al.* 2011), and potentially different drag forces due to
450   the whale's body exposure to air after the SLF, body buoyancy, and depth (Williams *et al.* 2000,
451   Goldbogen *et al.* 2006, Vennell *et al.* 2006). Although our minimal sample size must be
452   emphasized (n=1), our estimated body kinematics of the UAS filmed SLF event generally align
453   well with descriptions of lunge maneuvers by tagged rorquals at depth (Goldbogen *et al.* 2006,
454   Goldbogen *et al.* 2011), including discontinuation of fluking after strike and descriptions of
455   pectoral fin movements during the SLF event that may facilitate fine-scale steering toward the
456   prey patch (Cade *et al.* 2016, Segre *et al.* 2018).

457   The UAS footage enables unique observation of krill prey response to a whale predator. We
458   provide the first quantitative description of krill response distance and time to a foraging whale,
459   and we can qualitatively observe the krill evasion tactics as described by O'Brien (1987). It has
460   been theorized that larger rorquals are less maneuverable and thus require higher attack speed to
461   capture krill before their escape response (Potvin *et al.* 2010, Goldbogen *et al.* 2012). This
462   relationship is illustrated by the greater krill response distance during Event 4 (3.77 m) when the
463   whale was moving slower (2.69 m s^{-1}) than the SLF event (Table 1). The barrier between the
464   water's surface and air may play a role in rorqual SLF as krill response into air may be different
465   than in water. Based on the estimated response speed of dense surface schools of *N. australis* by
466   O'Brien (1987) of 20 cm s^{-1}, we can extrapolate our finding that krill flee 0.8 s prior to strike
467   (whale's mouth) to estimate that only krill within 16 cm of the edge of the whale's gape would
468   escape. We do not know the density of the targeted prey patch so we cannot estimate the amount
469   or percent of krill captured or escaped. However, this basic extrapolation demonstrates how
470   continued measurements of whale predation kinematics and prey response, through UAS, tags,
471   and other technologies, can facilitate improved models and understanding of predator efficiency
472   and predator-prey dynamics.

473   While it remains equivocal how rorquals detect prey aggregations at fine-scales (Torres 2017), it
474   has been hypothesized that vision informs foraging roll maneuvers (Goldbogen *et al.* 2013a) and
475   choices at scales < 30 m (Torres 2017), and that a whale's right eye is preferentially used to
476   coordinate maneuvers through the left hemisphere of the brain (Friedlaender *et al.* 2017). The
477   UAS footage shows evidence for all three hypotheses. Just prior to the SLF event, the blue whale
478   performs a pre-lunge roll to her left that allows her right eye to observe the krill patch. With this
479   visual information about prey structure, the whale then makes kinematic maneuvers to optimize
480   her krill strike vector to maximize prey engulfment, such as orientating her lower jaw with the
481   dense upper edge of the patch, modulating her gape size to conserve locomotor costs, and timing
482   her jaw opening at max speed to reduce startle response in the krill. Additional sensory
483   information may also have been used, potentially including passive listening to krill-produced
484   noise (Torres 2017) and tactile senses from vibrissae on the mandibles at close range (Torres
485   2017). However, the whale appears to use her right eye during all four UAS filmed events, which
486   demonstrates the importance of visual cues while foraging in these conditions and the whale's

487 ability to make quick behavioral choices likely based on krill patch size, orientation, distance and
488 density (Table 1).

489 At all depths, rorquals perform lunges with various approach maneuvers (Goldbogen *et al.* 2006,
490 Goldbogen *et al.* 2013a, Kot *et al.* 2014, Friedlaender *et al.* 2017), including 'regular lunges'
491 where the dorsal side faces the surface, and 'lateral lunges' that include a body roll to one side
492 (Goldbogen *et al.* 2006), such as observed in the UAS filmed whale. A whale's choice to
493 perform a lateral lunge at the surface may be due to good visual detection of a prey patch,
494 allowing the whale to orient its jaws so that the largest mouth dimension captures the maximum
495 patch. If patches are larger at depth where visual cues are reduced, mouth orientation relative to
496 the patch may be more challenging and not as critical, making regular lunges, perhaps using a
497 wider gape, more common. Although it has been proposed that blue whales are more likely to
498 roll to their left when feeding at shallow depths (Friedlaender *et al.* 2017), we suggest that the
499 UAS filmed whale chose to roll to her right so that the bend and orientation of the whale's body
500 during the lateral lunge corresponded to the prey patch. While eyeing the krill patch, the whale
501 could have continued on her left side, but this position would have led to an oblique intersection
502 with the krill patch and thus not maximized prey engulfment. Hence, pre-lunge rolls may inform
503 questions of lateralization (Friedlaender *et al.* 2017), and patch orientation to the whale may be a
504 driver of roll direction, at least when targeting shallow patchy prey with good visual cues.

505   Blue whale surface feeding has lower energetic costs than feeding at depth due to differences in
506 active metabolic rates (AMR), shorter transit cost between prey patches and the surface, and
507 shorter dive recovery times (variation in drag forces by water depth are not accounted for;
508 Goldbogen *et al.* 2011). Hence, when krill density is greater near the surface, such as in the STB
509 during our 2017 survey (Fig. 3), we should expect blue whales to forage more frequently near the
510 surface in order to optimize foraging efficiency. Even if surface krill patches are less dense,
511 surface feeding may still be energetically preferable over diving to feed on denser patches due to
512 relative energy gain (Doniol-Valcroze *et al.* 2011, Hazen *et al.* 2015). Goldbogen et al. (2011)
513 estimates that a 22 m long blue whale feeding on low krill density of 0.15 kg m^{-3} will have an
514 energetic efficiency of 7.9 (calculated as the ratio of energy gained from ingested krill divided by
515 all energy expenditures of the foraging dive including mechanical energy demands, AMR,
516 recovery time at the surface, and food assimilation costs relative to krill density). Based on the
517 smaller length of the UAS filmed whale (18.69 m) and that lunge feeding costs scale with body
518 size of rorquals due to mass specific engulfment capacity (Potvin *et al.* 2010, Goldbogen *et al.*
519 2012), the foraging efficiency of the UAS filmed SLF event was likely higher than 7.9.
520 Furthermore, the fact that the whale did not respire immediately after the SLF event indicates the
521 low energetic cost of the lunge. However, not all surface krill patches are energetically efficient
522 foraging opportunities, as demonstrated by Event 4 filmed by the UAS where the whale clearly
523 decides not to engage in a surface foraging lunge based on her perception of prey patch
524 characteristics (i.e., density, orientation), illustrating that blue whales maximize resource gain
525 relative to both prey availability and prey accessibility.

526

527 **Conclusions**

528   This study supports the hypothesis that surface feeding is an important component of New
529   Zealand blue whale foraging efficiency and we illustrate the utility of UAS to document these
530   surface behaviors. To fully understand how blue whales optimize foraging effort, surface feeding
531   events should be recorded and analyzed in conjunction with behaviors at depth, particularly in
532   regions where prey distribution patterns are unknown. Globally, blue whale populations exhibit
533   variation in morphology, behavior, and target prey species, which necessitates diversification of
534   blue whale study populations and ecosystems to obtain more complete knowledge of blue whale
535   foraging ecology. Blue whales have a large range of body length across sub-species (18-30 m),
536   show behavioral plasticity when foraging to balance krill consumed with energetic and diving
537   costs, and have maneuverability and foraging depth limitations that scale inversely, and
538   allometrically with body size (Potvin *et al.* 2010, Goldbogen *et al.* 2012, Goldbogen *et al.* 2017).
539   Through comparative studies of blue whale foraging strategies associated with different prey
540   ecology, ecosystems and functional body forms, we may improve our ecological understanding
541   and management capability. For instance, blue whales in Chile are 18.9 m to 22.1 m (Durban *et*
542   *al.* 2016), feed on a different krill species (Buchan and Quiñones 2016), have relatively high SLF
543   rates (Buchan and Quiñones 2016), and demonstrate shallow diving patterns (< 50 m;
544   Bocconcelli *et al.* 2016). Moreover, such diversity in foraging strategies may help explain the
545   evolutionary diversification of blue whale sub-species by better linking form and functional
546   ecology, such as the relatively small New Zealand blue whale that potentially sacrificed
547   engulfment size and diving capacity for increased agility to capture patchier surface prey.

548   Using UAS as our observational platform, we estimated the kinematics and prey response of a
549   blue whale's surface foraging events – behaviors that can be difficult to quantify in
550   accelerometer or camera tag data. We analyzed our UAS video footage of just four surface
551   foraging observations of one whale as a proof of concept, and were able to provide new
552   information on New Zealand blue whale foraging kinematics, energetics, sensory cues, and
553   predator-prey response dynamics. We suggest that incorporating UAS into studies of blue whale
554   foraging will complement tagging data by providing information on surface feeding rates,
555   kinematic coordination of fluke, pectoral fin, and mouth movements, and, when conditions are
556   favorable, the prey patch. UAS is a minimally invasive data collection technique (Christiansen *et*
557   *al.* 2016, Domínguez-Sánchez *et al.* 2018), and with increased replicate observations, it could be
558   an excellent tool to enhance our understanding of rorqual surface foraging ecology and prey
559   patch geometry and response to predation. Indeed, a recent study applied GoPro cameras and
560   UAS to improve descriptions of humpback whale oral morphology during surface feeding
561   (Werth *et al.* 2019). Although the current UAS battery life is typically limited to ~20 min,
562   operation of multiple UAS to alternate flight time with battery swaps could facilitate continuous
563   recording. Simultaneous measurements of prey and predator at fine-scales during feeding events
564   are rare but critical to understanding ecological processes and foraging efficiency (Goldbogen *et*
565   *al.* 2015), and whale-borne video tags (Calambokidis *et al.* 2007, Cade *et al.* 2016) and UAS can
566   fill this data gap. While more studies are needed to understand the complex interplay between
567   blue whales and their prey (Goldbogen *et al.* 2013a), we contend that application of different
568   technologies in a broader range of ecosystems would be highly beneficial.

569

Acknowledgements

570

571   The project was accomplished through the dedicated fieldwork of many individuals including the
572   crew of the *RV Star Keys* (Western Work Boats, Ltd.), Kristin Brooke Hodge, Mike Ogle, and
573   Callum Lilley. We are grateful to Kim Bernard and Pablo Escobar-Flores for assistance with
574   echosounder data analysis, to Kim Bernard and Daniel Palacios for constructive feedback on this
575   manuscript, and to David Cade and two anonymous reviewers for highly constructive and
576   insightful reviews that improved this manuscript.

577

578

References

Acevedo-Gutierrez, A., D. A. Croll and B. R. Tershy. 2002. High feeding costs limit dive time in the largest whales. Journal of Experimental Biology 205:1747-1753.

Allen, A. N., J. A. Goldbogen, A. S. Friedlaender and J. Calambokidis. 2016. Development of an automated method of detecting stereotyped feeding events in multisensor data from tagged rorqual whales. Ecology and Evolution 6:7522-7535.

Barlow, D. R., L. G. Torres, K. B. Hodge, D. Steel, C. S. Baker, T. E. Chandler, N. Bott, R. Constantine, M. C. Double, P. Gill, D. Glasgow, R. M. Hamner, C. Lilley, M. Ogle, P. A. Olson, C. Peters, K. A. Stockin, C. T. Tessaglia-Hymes and H. Klinck. 2018. Documentation of a New Zealand blue whale population based on multiple lines of evidence. Endangered Species Research 36:27-40.

Bernard, K. S., M. Cimino, W. Fraser, J. Kohut, M. J. Oliver, D. Patterson-Fraser, O. M. E. Schofield, H. Statscewich, D. K. Steinberg and P. Winsor. 2017. Factors that affect the nearshore aggregations of Antarctic krill in a biological hotspot. Deep Sea Research Part I: Oceanographic Research Papers 126:139-147.

Bernard, K. S. and D. K. Steinberg. 2013. Krill biomass and aggregation structure in relation to tidal cycle in a penguin foraging region off the Western Antarctic Peninsula. ICES Journal of Marine Science 70:834-849.

Bocconcelli, A., L. Hickmott, G. Chiang, P. Bahamonde, G. Howes, R. Landea-Briones, F. Caruso, M. Saddler and L. Sayigh. 2016. DTAG studies of blue whales (*Balaenoptera musculus*) in the Gulf of Corcovado, Chile. Proceedings of meetings on acoustics 27:040002.

Buchan, S. J. and R. A. Quiñones. 2016. First insights into the oceanographic characteristics of a blue whale feeding ground in northern Patagonia, Chile. Marine Ecology Progress Series 554:183-199.

Burnett, J. D., L. Lemos, D. R. Barlow, M. G. Wing, T. E. Chandler and L. G. Torres. 2018. Estimating morphometric attributes of baleen whales with photogrammetry from small UAS: A case study with blue and gray whales. Marine Mammal Science:1-32.

Cade, David E., Ari S. Friedlaender, J. Calambokidis and Jeremy A. Goldbogen. 2016. Kinematic diversity in rorqual whale feeding mechanisms. Current Biology 26:2617-2624.

Calambokidis, J., G. S. Schorr, G. H. Steiger, J. Francis, M. Bakhtiari, G. Marshall, E. M. Oleson, D. Gendron and K. Robertson. 2007. Insights into the underwater diving, feeding, and calling behavior of blue whales from a suction-cup-attached video-imaging tag (CRITTERCAM). Marine Technology Society Journal 41:19-29.

Charnov, E. L. 1976. Optimal foraging: The marginal value theorem. Theoretical Population Biology 9:129-136.

Christiansen, F., L. Rojano-Doñate, P. T. Madsen and L. Bejder. 2016. Noise levels of multi-rotor unmanned aerial vehicles with implications for potential underwater impacts on marine mammals. Frontiers in Marine Science 3, 277.

Comer, R., G. Kinn, D. Light and C. Mondello. 1998. Talking digital. Photogrammetric Engineering and Remote Sensing 64:1139-1142.

Corkeron, P. J., P. Ensor and K. Matsuoka. 1999. Observations of blue whales feeding in Antarctic waters. Polar Biology 22:213-215.

Croll, D. A., A. Acevedo-Gutiérrez, B. R. Tershy and J. Urbán-Ramírez. 2001. The diving behavior of blue and fin whales: is dive duration shorter than expected based on oxygen

625   stores? Comparative Biochemistry and Physiology PartA: Molecular and integrative
626   Physiology 129:797-809.
627 Croll, D. A., B. Marinovic, S. Benson, F. P. Chavez, N. Black, R. Ternullo and B. R. Tershy.
628   2005. From wind to whales: trophic links in a coastal upwelling system. Marine Ecology
629   Progress Series 289:117-130.
630 Dawson, S. M., M. H. Bowman, E. Leunissen and P. Sirguey. 2017. Inexpensive aerial
631   photogrammetry for studies of whales and large marine animals. Frontiers in Marine
632   Science 4, 366.
633 Domínguez-Sánchez, C. A., K. A. Acevedo-Whitehouse and D. Gendron. 2018. Effect of
634   drone-based blow sampling on blue whale (*Balaenoptera musculus*) behavior. Marine
635   Mammal Science 0.
636 Doniol-Valcroze, T., V. Lesage, J. Giard and R. Michaud. 2011. Optimal foraging theory
637   predicts diving and feeding strategies of the largest marine predator. Behavioral Ecology
638   22:880-888.
639 Durban, J. W., M. J. Moore, G. Chiang, L. S. Hickmott, A. Bocconcelli, G. Howes, P. A.
640   Bahamonde, W. L. Perryman and D. J. LeRoi. 2016. Photogrammetry of blue whales
641   with an unmanned hexacopter. Marine Mammal Science 32:1510-1515.
642 Fiedler, P. C., S. B. Reilly, R. P. Hewitt, D. Demer, V. A. Philbrick, S. Smith, W. Armstrong, D.
643   A. Croll, B. R. Tershy and B. R. Mate. 1998. Blue whale habitat and prey in the
644   California Channel Islands. Deep-Sea Research II 45:1781-1801.
645 Friedlaender, A. S., E. L. Hazen, J. A. Goldbogen, A. K. Stimpert, J. Calambokidis and B. L.
646   Southall. 2016. Prey-mediated behavioral responses of feeding blue whales in controlled
647   sound exposure experiments. Ecological Applications 26:1075-1085.
648 Friedlaender, A. S., E. L. Hazen, D. P. Nowacek, P. N. Halpin, C. Ware, M. T. Weinrich, T.
649   Hurst and D. Wiley. 2009. Diel changes in humpback whale *Megaptera novaeangliae*
650   feeding behavior in response to sand lance Ammodytes spp. behavior and distribution.
651   Marine Ecology Progress Series 395:91-100.
652 Friedlaender, A. S., J. E. Herbert-Read, E. L. Hazen, D. E. Cade, J. Calambokidis, B. L. Southall,
653   A. K. Stimpert and J. A. Goldbogen. 2017. Context-dependent lateralized feeding
654   strategies in blue whales. Current Biology 27:R1206-R1208.
655 Gill, P. C. 2002. A blue whale (*Balaenoptera musculus*) feeding ground in a southern Australian
656   coastal upwelling zone. Journal of Cetacean Research and Management 4:179-184.
657 Goldbogen, J. A., D. E. Cade, J. Calambokidis, A. S. Friedlaender, J. Potvin, P. S. Segre and A.
658   J. Werth. 2017. How baleen whales feed: The biomechanics of engulfment and filtration.
659   Annual Review of Marine Science 9:367-386.
660 Goldbogen, J. A., J. Calambokidis, D. A. Croll, J. T. Harvey, K. M. Newton, E. M. Oleson, G.
661   Schorr and R. E. Shadwick. 2008. Foraging behavior of humpback whales: kinematic and
662   respiratory patterns suggest a high cost for a lunge. Journal of Experimental Biology
663   211:3712-3719.
664 Goldbogen, J. A., J. Calambokidis, D. A. Croll, M. F. McKenna, E. Oleson, J. Potvin, N. D.
665   Pyenson, G. Schorr, R. E. Shadwick and B. R. Tershy. 2012. Scaling of lunge-feeding
666   performance in rorqual whales: mass-specific energy expenditure increases with body
667   size and progressively limits diving capacity. Functional Ecology 26:216-226.
668 Goldbogen, J. A., J. Calambokidis, A. S. Friedlaender, J. Francis, S. L. DeRuiter, A. K. Stimpert,
669   E. Falcone and B. L. Southall. 2013a. Underwater acrobatics by the world's largest
670   predator: 360° rolling manoeuvres by lunge-feeding blue whales. Biology Letters 9.

671 Goldbogen, J. A., J. Calambokidis, E. Oleson, J. Potvin, N. D. Pyenson, G. Schorr and R. E.
672   Shadwick. 2011. Mechanics, hydrodynamics and energetics of blue whale lunge feeding:
673   efficiency dependence on krill density. Journal of Experimental Biology 214:131-146.
674 Goldbogen, J. A., J. Calambokidis, R. E. Shadwick, E. M. Oleson, M. A. McDonald and J. A.
675   Hildebrand. 2006. Kinematics of foraging dives and lunge-feeding in fin whales. Journal
676   of Experimental Biology 209:1231-1244.
677 Goldbogen, J. A., E. L. Hazen, A. S. Friedlaender, J. Calambokidis, S. L. DeRuiter, A. K.
678   Stimpert, B. L. Southall and D. Costa. 2015. Prey density and distribution drive the
679   three-dimensional foraging strategies of the largest filter feeder. Functional Ecology
680   29:951-961.
681 Goldbogen, J. A., B. L. Southall, S. L. DeRuiter, J. Calambokidis, A. S. Friedlaender, E. L.
682   Hazen, E. A. Falcone, G. S. Schorr, A. Douglas, D. J. Moretti, C. Kyburg, M. F.
683   McKenna and P. L. Tyack. 2013b. Blue whales respond to simulated mid-frequency
684   military sonar. Proceedings of the Royal Society of London. Series B: Biological
685   Sciences 280.
686 Hazen, E. L., A. S. Friedlaender and J. A. Goldbogen. 2015. Blue whales (*Balaenoptera*
687   *musculus*) optimize foraging efficiency by balancing oxygen use and energy gain as a
688   function of prey density. Science Advances 1.
689 Koo, T. K. and M. Y. Li. 2016. A guideline of selecting and reporting intraclass correlation
690   coefficients for reliability research. Journal of Chiropractic Medicine 15:155-163.
691 Kot, B. W., R. Sears, D. Zbinden, E. Borda and M. S. Gordon. 2014. Rorqual whale
692   (Balaenopteridae) surface lunge-feeding behaviors: Standardized classification, repertoire
693   diversity, and evolutionary analyses. Marine Mammal Science 30:1335-1357.
694 Kramer, D. L. 1988. The behavioral ecology of air breathing by aquatic animals. Canadian
695   Journal of Zoology 66:89-94.
696 Krützen, M., L. M. Barré, L. M. Möller, M. R. Heithaus, C. Simms and W. B. Sherwin. 2002. A
697   biopsy system for small cetaceans: darting success and wound healing in *Tursiops* spp.
698   Marine Mammal Science 18:863-878.
699 Ladroit, Y. 2017. ESP3. NIWA, Wellington, New Zealand.
700 Lawson, G. L., P. H. Wiebe, T. K. Stanton and C. J. Ashjian. 2008. Euphausiid distribution along
701   the Western Antarctic Peninsula—Part A: Development of robust multi-frequency
702   acoustic techniques to identify euphausiid aggregations and quantify euphausiid size,
703   abundance, and biomass. Deep-Sea Research Part II: Topical Studies in Oceanography
704   55:412-431.
705 McKenna, M. F., J. Calambokidis, E. M. Oleson, D. W. Laist and J. A. Goldbogen. 2015.
706   Simultaneous tracking of blue whales and large ships demonstrates limited behavioral
707   responses for avoiding collision. Endangered Species Research 27:219-232.
708 Nickels, C. F., L. M. Sala and M. D. Ohman. 2019. The euphausiid prey field for blue whales
709   around a steep bathymetric feature in the southern California current system. Limnology
710   and Oceanography 64:390-405.
711 O'Brien, D. P. 1987. Description of escape responses of krill (Crustacea: Euphausiacea), with
712   particular reference to swarming behavior and the size and proximity of the predator.
713   Journal of Crustacean Biology 7:449-457.
714 O'Brien, D. P. 1988. Surface schooling behaviour of the coastal krill *Nyctiphanes australis*
715   (Crustacea: Euphausiacea) off Tasmania, Australia. Marine Ecology Progress Series
716   42:219-233.

717   Orians, G. H. 1979. On the theory of central place foraging. Pages 157-177   Analysis of
718   ecological systems. Ohio State University Press.
719   Owen, K., R. A. Dunlop, J. P. Monty, D. Chung, M. J. Noad, D. Donnelly, A. W. Goldizen and
720   T. Mackenzie. 2016. Detecting surface-feeding behavior by rorqual whales in
721   accelerometer data. Marine Mammal Science 32:327-348.
722   Owen, K., A. S. Kavanagh, J. D. Warren, M. J. Noad, D. Donnelly, A. W. Goldizen and R. A.
723   Dunlop. 2017. Potential energy gain by whales outside of the Antarctic: prey preferences
724   and consumption rates of migrating humpback whales (*Megaptera novaeangliae*). Polar
725   Biology 40:277-289.
726   Potvin, J., J. A. Goldbogen and R. E. Shadwick. 2010. Scaling of lunge feeding in rorqual
727   whales: An integrated model of engulfment duration. Journal of Theoretical Biology
728   267:437-453.
729   R Development Core Team. 2018. R: A language and environment for statistical computing. R
730   Foundation for Statistical Computing, Vienna, Austria.
731   Schoenherr, J. R. 1991. Blue whales feeding on high concentrations of euphausiids around
732   Monterey Submarine Canyon. Canadian Journal of Zoology 69:583-594.
733   Segre, P. S., D. E. Cade, J. Calambokidis, F. E. Fish, A. S. Friedlaender, J. Potvin and J. A.
734   Goldbogen. 2018. Body flexibility enhances maneuverability in the world's largest
735   predator. Integrative and Comparative Biology 59:48-60.
736   Torres, L. G. 2013. Evidence for an unrecognised blue whale foraging ground in New Zealand.
737   New Zealand Journal of Marine and Freshwater Research 47:235-248.
738   Torres, L. G. 2017. A sense of scale: Foraging cetaceans' use of scale-dependent multimodal
739   sensory systems. Marine Mammal Science 33:1170-1193.
740   Torres, L. G., S. L. Nieukirk, L. Lemos and T. E. Chandler. 2018. Drone up! Quantifying whale
741   behavior from a new perspective improves observational capacity. Frontiers in Marine
742   Science 5.
743   Vennell, R., D. Pease and B. Wilson. 2006. Wave drag on human swimmers. Journal of
744   Biomechanics 39:664-671.
745   Ware, C., A. S. Friedlaender and D. P. Nowacek. 2011. Shallow and deep lunge feeding of
746   humpback whales in fjords of the West Antarctic Peninsula. Marine Mammal Science
747   27:587-605.
748   Werth, A. J., M. M. Kosma, E. M. Chenoweth and J. M. Straley. 2019. New views of humpback
749   whale flow dynamics and oral morphology during prey engulfment. Marine Mammal
750   Science 0.
751   Williams, T. M., R. W. Davis, L. A. Fuiman, J. Francis, B. J. Le, Boeuf, M. Horning, J.
752   Calambokidis and D. A. Croll. 2000. Sink or swim: Strategies for cost-efficient diving by
753   marine mammals. Science 288:133-136.
754   Williams, T. M., J. Haun, R. W. Davis, L. A. Fuiman and S. Kohin. 2001. A killer appetite:
755   metabolic consequences of carnivory in marine mammals. Comparative Biochemistry
756   and Physiology PartA: Molecular and integrative Physiology 129:785-796.
757   Young, J., A. Jordan, C. Bobbi, R. Johannes, K. Haskard and G. Pullen. 1993. Seasonal and
758   interannual variability in krill (*Nyctiphanes australis*) stocks and their relationship to the
759   fishery for jack mackerel (*Trachurus declivis*) off eastern Tasmania, Australia. Marine
760   Biology 116:9-18.

761

Description the four blue whale (*B. m. brevicauda*) surface events filmed via Unmanned Aerial Systems (UAS) on 20-Feb-2017 in the South Taranaki Bight, New Zealand, including comparative metrics of speed, and krill patch size and response to whale.

Event	Local start time	Whale behavior	Krill patch size (m^2)	Distance (m) at which whale responds to krill patch (time from intersection/ strike)	Maximum speed (m s^{-1})	Distance (m) between krill patch and whale when krill first show flee response	Speed (m s^{-1}) of whale when krill respond	Distance from eye to krill patch (m) when whale visually inspects patch (time from intersection/strike)
1	19:23:38	Whale engages in surface lunge feeding event	45	20.74 (9.0)	3.33	2.00	3.00	18.46 (6.5)
2	19:30:19	Whale flares pectoral fins to alter course slightly as she investigates a small krill patch and surfaces - no feeding	1	17.87 (6.45)	2.75	NA	NA	11.35 (2.44)
3	19:36:36	Whale surfaces and makes a slight course change near small krill patches - no feeding	2.47	5.02 (NA)	NA	4.93	NA	8.56 (NA)

| 4 | 19:38:05 | Whale flares pectoral fins, changes speed, and rotates her body to examine a medium size krill patch - no feeding | 4.72 | 12.29 (4.83) | 2.90 | 3.77 | 2.69 | 15.24 (4.5) |

Comparison of krill (*Nyctiphanes australis*) aggregation depth in the South Taranaki Bight, New Zealand, not within 2 km radius of blue whale (*B. m. brevicauda*) sightings and those within 2 km of sightings.

The mean dive time of whales at each sighting by group (all, foraging observed, surface lunge feeding observed) are also given.

2   [1]The number of dives monitored to assess mean dive time was not maintained for four out of 32

3   blue whale sightings, although the mean dive time at all sightings was recorded. Therefore, a

	Sample size (blue whale sightings/ krill aggregations)	Mean krill depth (m); (SE)	Mean dive time (min) (SE); n=# of dives
All krill aggregations not at sighting	NA / 2009	47.31 (±0.71)	NA
All sightings	32 / 874	38.09 (±0.92)	2.83 (±0.18); n > 248[1]
All foraging sightings	15 / 392	32.64 (±1.27)	2.56 (±0.19); n>137[2]
Sightings with surface lunge feeding observed	6 / 122	26.42 (±2.01)	1.77 (±0.07); n=80

4   minimum sample size of dives monitored (n = 248) is provided.

5   [2]The number of dives monitored to assess mean dive time was not maintained for two out of 15

6   foraging blue whale sightings, although the mean dive time at all sightings was recorded.

7   Therefore, a minimum sample size of dives monitored (n = 137) at foraging sightings is

8   provided.

Figure 1

Blue whale survey tracklines and sighting locations.

Survey tracklines in 2017 in the South Taranaki Bight (STB) with locations of blue whale sightings, and where surface lunge feeding was observed, denoted. Inset map shows location of the STB within New Zealand.
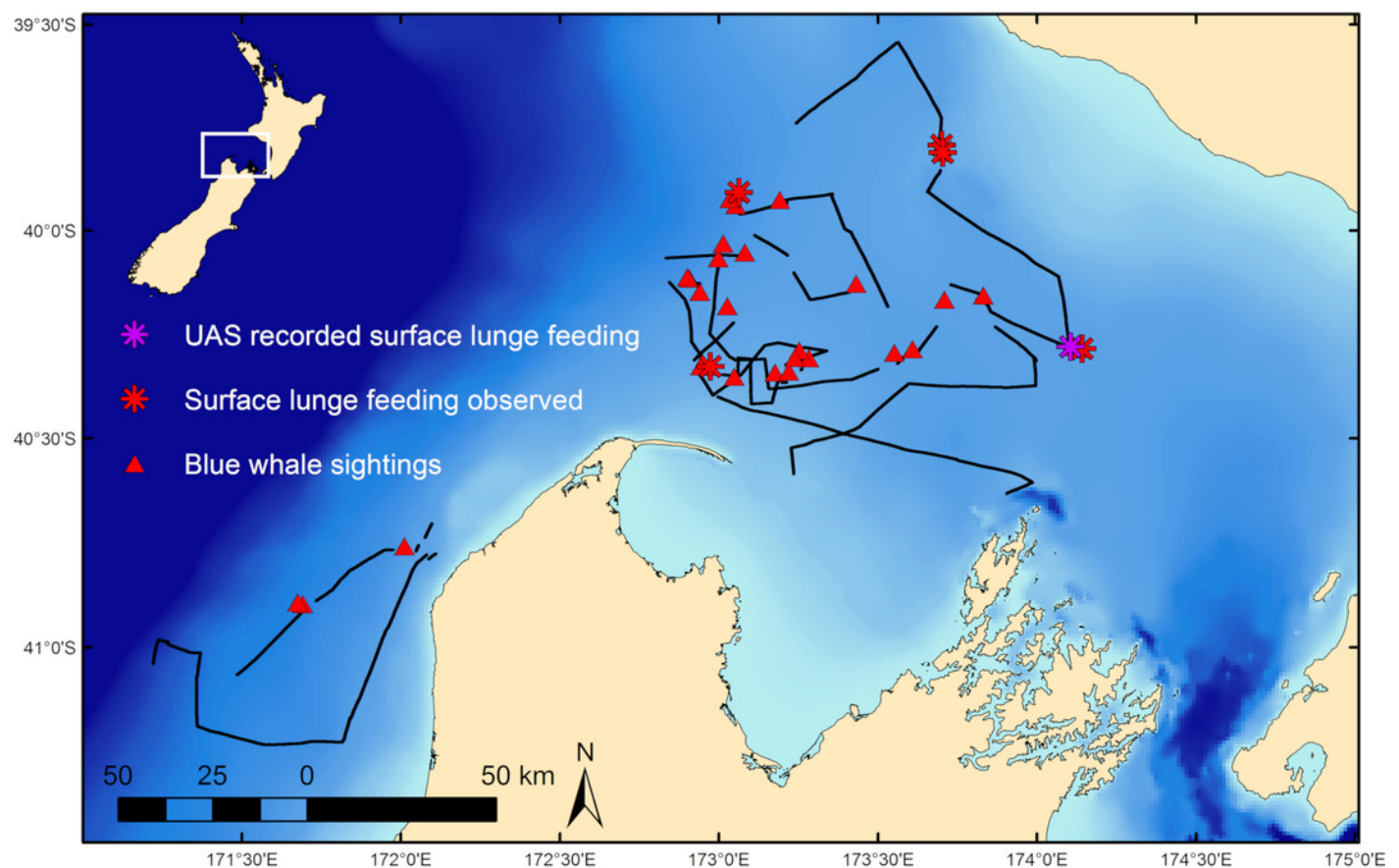
Figure 2

Body kinematics, and corresponding still images, during blue whale surface lunge feeding event derived from Unmanned Aerial Systems (UAS) image analysis.

(a) Mean head inclination and roll (with CV in shaded areas), (b) relative speed and acceleration, and (c) distance from the tip of the whale's rostrum to the nearest edge of krill patch. Blue line on plots indicate when krill first respond to the predation event, and the purple dashed lines indicate strike at time = 0. The orange lines indicate the time at which the whale's gape is widest, head inclination is maximum, and deceleration is greatest. (d) Image of whale eyeing krill patch with measured distance between eye and patch. (e) Image taken when krill begin to respond to predation event. (f) Image illustrating krill flee response. (g) Image of widest gape and angle measurement. Comparative images of krill patch size and density (h) pre- and (i) post-strike. Comparative images of head inclination (j) 2 sec pre-strike, (k) at strike, and (l) post-strike of surface lunge feeding event (Example roll images in Fig. S2). Images in d-l are cropped to enhance illustrations (raw video available in Supplemental Information). All images captured at 30 m altitude.
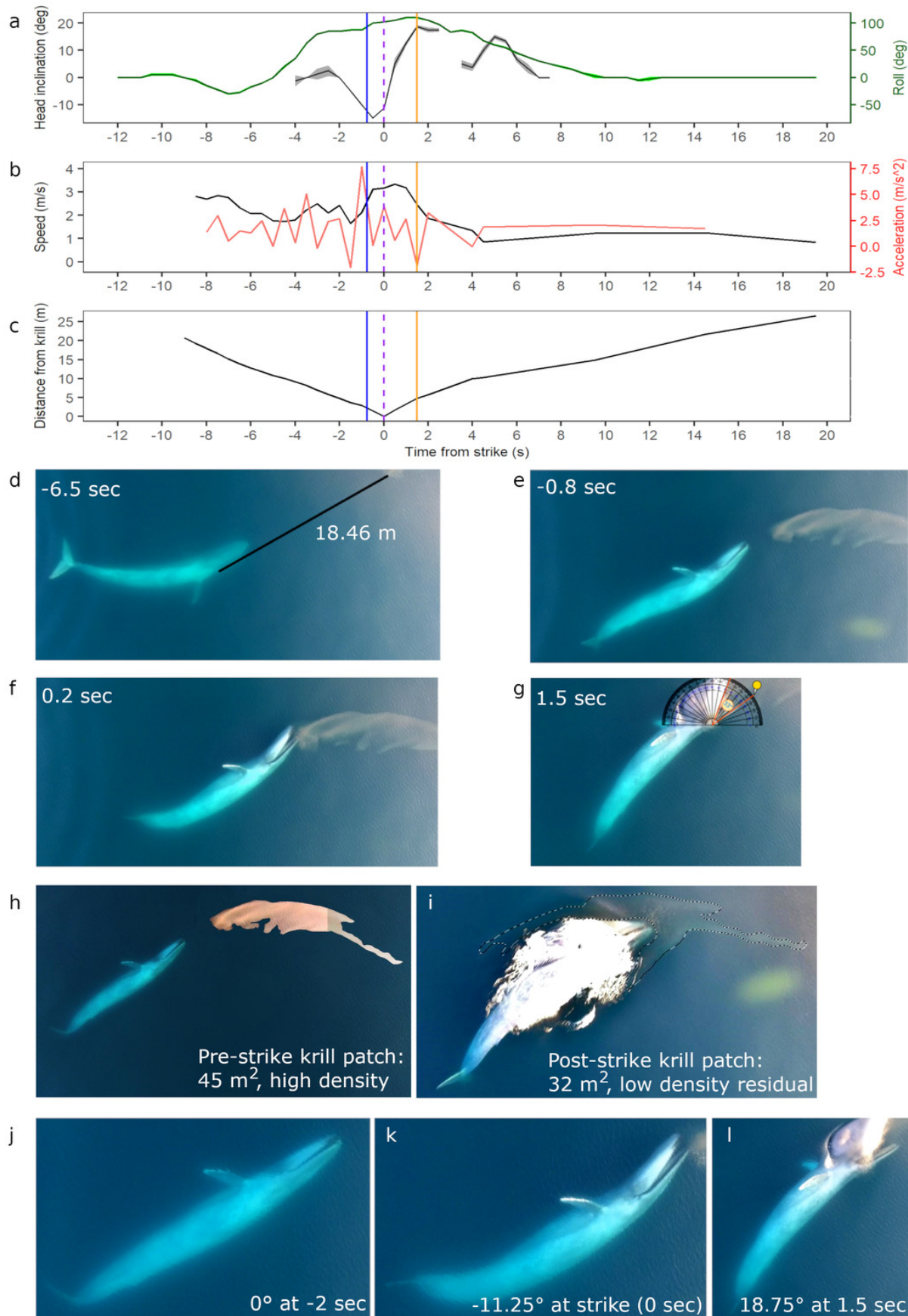
Figure 3

Density contours comparing the depth and density (Sv) of krill aggregations at blue whale foraging sightings (red shading) and in absence of blue whales (grey shading).

Density contours: 25% = darkest shade, 75% = medium shade, 95% = light shade. Blue circles indicate krill aggregations detected within 2 km of the sighting of the UAS filmed surface foraging whale analyzed in this study.
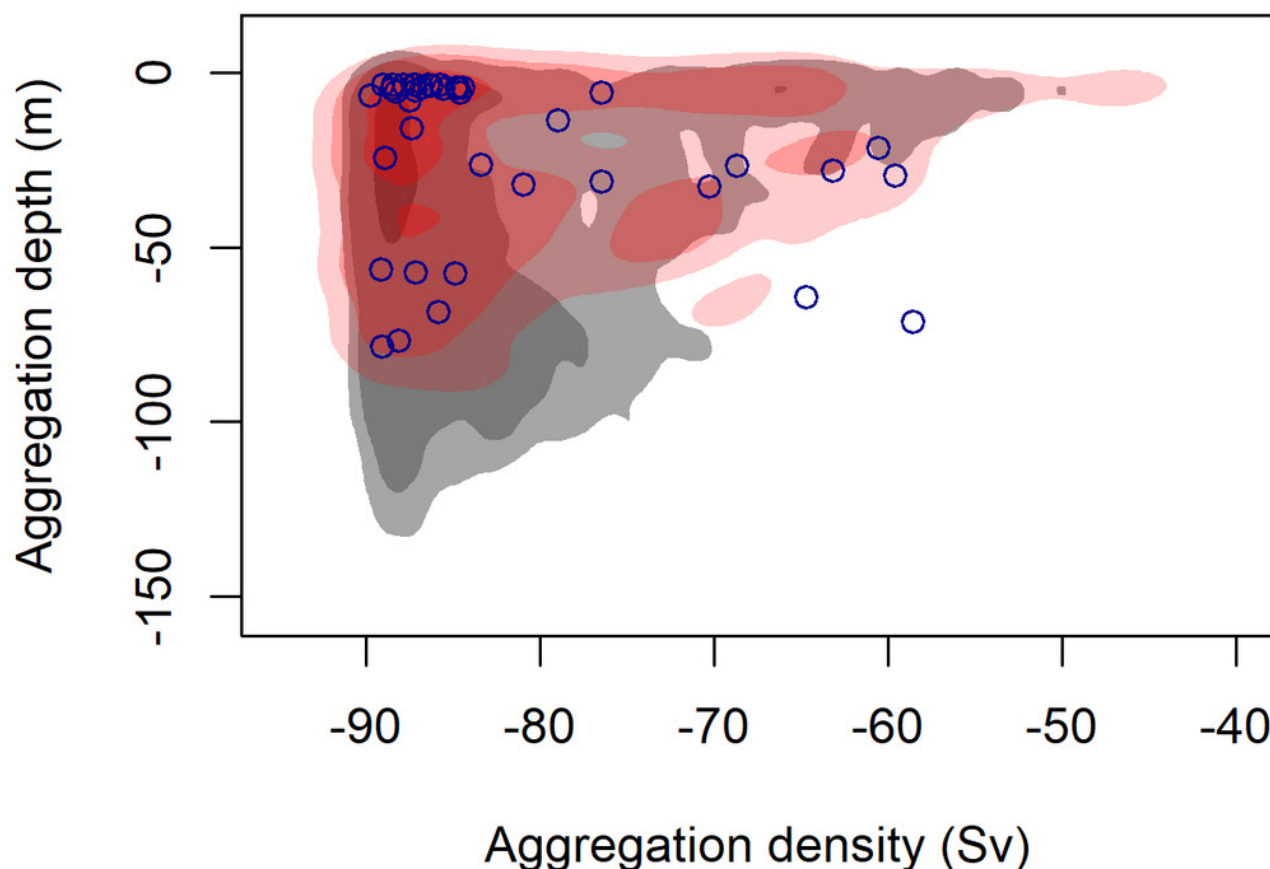
Figure 4

Still images from UAS video of three separate surface blue whale foraging events captured when it was estimated that the whale visually detects the krill patch with her right eye.

Measured distances between the eye and closest edge of krill patch are given for event 1 (a), event 2 (b) and event 3 (c). See Table 2 for details.